Collision-induced desorption in 193-nm photoinduced reactions in (O_2+CO) adlayers on Pt(112)

Song Han
Graduate School of Environmental Earth Science, Hokkaido University, Sapporo 060-0811, Japan

Yunsheng Ma and Tatsuo Matsushima[a)]
Catalysis Research Center, Hokkaido University, Sapporo 001-0021, Japan

(Received 16 December 2004; accepted 29 June 2005; published online 6 September 2005)

The spatial distribution of desorbing O_2 and CO_2 was examined in 193-nm photoinduced reactions in O_2+CO adlayers on stepped Pt (112)=[(*s*)3(111)×(001)]. The O_2 desorption collimated in inclined ways in the plane along the surface trough, confirming the hot-atom collision mechanism. In the presence of CO(*a*), the product CO_2 desorption also collimated in an inclined way, whereas the inclined O_2 desorption was suppressed. The inclined O_2 and CO_2 desorption is explained by a common collision-induced desorption model. At high O_2 coverage, the CO_2 desorption collimated closely along the (111) terrace normal. © *2005 American Institute of Physics*.
[DOI: 10.1063/1.2006678]

I. INTRODUCTION

Collimated fragment desorption from surface molecules has frequently been reported in electron-stimulated desorption ion angular distribution (ESDIAD), in which the emission is initiated by the injection of electrons or photons.[1–3] The desorption collimates along the ruptured bond axis, yielding structural information of adsorbed molecules in the fragment spatial distribution. However, the collimation is different when "hot atoms" are emitted by the injection. Such hot-atom-mediated desorption has been studied in only a few cases, and the energy-transfer mechanism remains unclear.[4] This paper delivers detailed desorption studies of oxygen in 193-nm photoinduced reactions in O_2+CO adlayers on stepped Pt(112)=[(*s*)3(111)×(001)]. The O_2 desorption collimated in inclined ways in the plane along the surface trough, confirming the hot-atom collision mechanism. In the presence of CO, the product CO_2 desorption also collimated in a similar inclined way at low CO coverage. On the other hand, the CO_2 or O_2 desorption collimated closely along the (111) terrace normal at high $O_2(a)$ coverage.

In thermal reactions of adsorbed molecules, collimated product desorption has been limited to associative processes, such as $CH_3(a)+H(a)\rightarrow CH_4(g)$ and $CO(a)+O(a)\rightarrow CO_2(g)$.[5] The product molecule is usually bulky and likely to be repelled by the surface at the moment of formation, showing hyperthermal energy. Its desorption collimates fairly along the local normal of the product formation site. In the thermal decomposition of adsorbed molecules, the released fragment has been believed to be quickly thermalized to the surface temperature before desorption, however, few reports are available.[6–8] Thus, the recently reported inclined N_2 emission in N_2O decomposition on Pd(110), Rh(110), and Ir(110) is the first example to show *collimated fragment desorption in thermal decompositions* on solid surfaces.[9–13] The energy-transfer mechanism to the product N_2 is not clear, however, there is a close similarity in the inclined desorption between the above photodesorbed O_2 and the N_2 in the N_2O decomposition.[14] In both cases, desorbing products have high kinetic energy, and their emission collimates in a highly inclined way in the plane along the axis of parent molecules. Thus, the photoinduced process can provide a good model system yielding directed desorption, in which the energy to initiate the reaction can be controlled.

There are clear differences in the mechanism between thermal and photoinduced CO oxidation. In the former, mobile-adsorbed CO molecules react with thermalized oxygen atoms to produce CO_2. One exceptional case was found for α-CO_2 formation, in which a hot-atom oxygen was proposed to be reactant through the thermal reaction.[5,8] On the other hand, in the photoinduced reaction, adsorbed O_2 emits hot-atom oxygen, which attacks CO(*a*).[15] The light is believed to be first absorbed by the metal, yielding excited electrons, which are trapped in the definite states of $O_2(a)$ and lead to its dissociation.[16,17] The product oxygen atoms are expected to be emitted along the ruptured bond axis of the parent $O_2(a)$, being able to induce directed-collision reactions; however, the amount of charge on it is not clear. Such an idea was first examined in photoinduced O_2 desorption on Ag(110) at 248-nm light by Zhu and co-worker[18,19] since O_2 is oriented along the $[1\bar{1}0]$ direction.[20] The observed directed desorption in an inclined way, however, was too small to be characterized. The O_2 desorption on Ag(110) was mostly collimated along the surface normal. Later, clearly directed (and inclined) desorption of CO_2 and O_2 was successfully designed on stepped Pt(113) on which O_2 was mostly oriented along the surface trough.[21–23] However, later low-energy electron diffraction (LEED) and scanning tunnelling microscope (STM) results showed that the surface was reconstructed into the (1×2) missing-row structure as [(*s*)3(111)×3(001)].[24,25] The surface structure after

[a)]Author to whom correspondence should be addressed. Fax:+81-11-706-9120; electronic mail: tatmatsu@cat.hokudai.ac.jp

$CO+O_2$ adsorption is not clear because their reconstruction is lifted by CO adsorption. Recently, Zeiri and co-worker reported their results for a molecular-dynamics (MD) simulation which was planned to explain the O_2 desorption at 248 nm on Ag(110).[26,27] In their simulations, strong coupling of surface corrugation and adsorbate-frustrated rotation as well as hot-atom energy plays a main role to control the collimation angle. The resultant O_2 desorption broadly collimates at either 20°–40° or 60°–80° off the surface normal toward the $[1\bar{1}0]$ direction at low O_2 density and the 10°–25° off normal desorption is enhanced at high density. No normally directed component was reproduced even at high density. Neither was the inclined CO_2 desorption discussed although it shows the interaction with the surface more clearly.

The purpose of this work is to examine, on a stable stepped surface, the hot-atom collision-induced desorption. The present surface is stable, consisting of three-atom-wide terraces with a (111) structure declining 19.5° from the bulk surface normal and two-atom-wide steps with a (001) structure inclined 35.2° in the opposite direction.[28] On Pt(112), oxygen admolecules lie along the surface trough in a wide coverage range.[29] The results at 193 nm nicely confirmed both the collimation angles and the energy dependence of the reaction cross section in the above MD simulations although some disagreements were clear. The inclined O_2 desorption on Pt(112) was once examined at 308 nm, where the desorption along the trough collimated around 40°.[30] However, the peak separation from the normally directed component was poor because of the low velocity of desorbing O_2.

II. EXPERIMENTS

The experiments were carried out in an ultrahigh-vacuum apparatus consisting of three chambers separately pumped.[31] A reaction chamber was equipped with LEED-Auger electron spectroscopy (AES) optics, an ion gun, and a quadruple mass (QM) spectrometer for angle-integrated (AI) desorption analysis. The collimator had a slit on each end, and the analyzer had another QM for angle-resolved (AR) measurements. The distance from the ionizer in the analyzer to the sample surface was 135 mm. A Pt(112) crystal (10 mm in diameter) was rotated to change the desorption angle (θ; polar angle). This angle was scanned in the normally directed plane either perpendicular to the surface trough or parallel to it. The angle is designated as θ_a in the former and θ_b in the latter. Here, the sign of the desorption angle is defined as positive so that the (111) terrace normal is $\theta_a=+19.5°$ (Fig. 1).

The crystal was cleaned by repeated Ar^+ bombardments and heating in oxygen of 6.7×10^{-6} Pa at the surface temperature (T_S) of 850 K. After flashing to 1200 K, the surface showed a sharp (1×1) LEED pattern. The clean surface was first exposed to $^{16}O_2$ and then $^{13}C^{18}O$ at $T_S=100$ K. Hereafter, ^{13}C and ^{18}O are simply referred to as C and O in the text. A nonpolarized 193-nm ArF laser (Lambda-Physics, Compex 100) pulse with a fluence of about 2 mJ/cm^2 was introduced to the sample with a repetition rate of 5 Hz. The transient surface temperature increase was estimated to be 2 K only, yielding no thermal effect for the O_2 dissociation and CO oxidation.[32] This adsorption-irradiation procedure was repeated five to ten times for a tolerable time-of-flight (TOF) spectrum. The surface was flashed after each run.

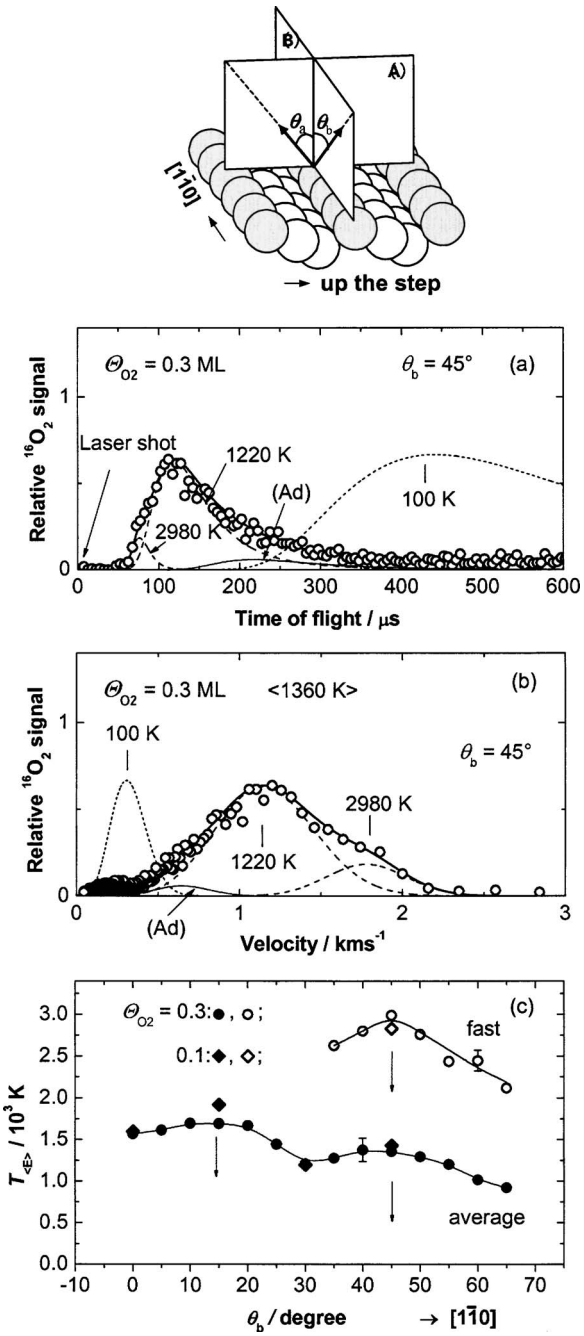

FIG. 1. (a) A typical time-of-flight spectrum of desorbing $^{16}O_2$ at $\theta_b=45°$ and $\Theta_{O_2}=0.3$ ML. (b) Velocity distribution derived from TOF in (a). A deconvolution is shown by broken curves. (Ad) is explained in the text. The translational temperature of each component is given. The value in $\langle\ \rangle$ indicates the average value. The dotted curve with 100 K represents a Maxwellian distribution at the surface temperature. (c) Translational temperatures of desorbing $^{16}O_2$ vs desorption angle. The "fast" was derived from velocity analysis. The desorption angles on Pt(112) are defined on the top. Plane (A) is perpendicular to the trough, and plane (B) is along the trough in the $[1\bar{1}0]$ direction. The desorption angles, θ_a and θ_b, are measured from the surface normal in these planes.

The light incidence angle was concomitantly scanned against the surface plane with the desorption angle because the angle between the light incidence and the analyzer axis

was fixed at 38°. The incidence angle was limited to between −45° and +45° from the bulk surface normal. The quantum yield is insensitive to the incident angle in this range for the photoinduced dissociation and desorption of oxygen.[33] The coverage of each species, Θ_{CO}, Θ_O, and Θ_{O_2} was first determined as the Al-thermal desorption spectroscopy (TDS) peak area relative to the maximum value and converted to the ratio of the species to the surface atoms by referring to the literature value.[28,34]

III. RESULTS

A. General features

The amount of adsorbed $O_2(a)$ and $CO(a)$ decreased during irradiation. This decrease was followed by postirradiation TDS. The amount of the remaining oxygen showed a first-order decay and yielded a photodesorption cross section of about 3×10^{-19} cm.[15,33] In $O_2(a)+CO(a)$ adlayers, desorption of both CO_2 and O_2 was induced by the irradiation, but no CO desorption was found. In most of the experiments, irradiation was continued to about 30% desorption of the initial amount of O_2. The flux of desorbed CO_2 and O_2 was determined from their TOF spectra. The angular distributions of desorbing O_2 and CO_2 depended on the reactant coverage and the crystal azimuth.

B. O_2 desorption

A typical TOF spectrum of desorbing oxygen in the photodesorption is shown in Fig. 1(a). In the experiments, the laser was fired 500 ms after the scan of a multichannel scalar (MCS) started. The ion drift time in the QM was separately determined and the arrival time was corrected. The resultant velocity distribution of desorbing O_2 at $\theta_b=45°$ is plotted in Fig. 1(b). In the velocity analysis, the contribution from the thermalized component described by a Maxwellian form at the surface temperature was first subtracted. This component was negligible without $CO(a)$ but became noticeable in the presence of $CO(a)$. The resulting distribution cannot be described by a single modified Maxwell distribution expressed as $f(\nu)=\nu^3\exp\{-(\nu-\nu_0)^2/\alpha^2\}$, where $f(\nu)$ is the distribution function, ν is the velocity of the molecule, ν_0 is the stream velocity, and α is the width parameter. When the desorption angle was above 30°, the observed distributions showed an additional higher-velocity component. Thus, the distribution was deconvoluted into *two* modified Maxwellian components in the way previously described.[35] A typical deconvolution is shown by broken curves. A shift from the observed curve is noticeable for this deconvolution into two components, as drawn by an extra tiny solid curve designated by (Ad). A better fitting was found when *three* components were considered. However, a unique deconvolution became difficult because of six parameters although the fraction of the major components was hardly affected.

The average kinetic energy was first calculated from the distribution without deconvolution and is shown in the temperature unit as $T_{\langle E\rangle}=\langle E\rangle/2k$, where $\langle E\rangle$ is the mean translational energy and k is the Boltzmann constant [Fig. 1(c)]. With O_2 coverage of 0.3 monolayer (ML), the average translational temperature peaked to 1700 K at $\theta_b=10°-20°$ and to 1360 K at $\theta_b=40°-45°$, indicating two collimation angles. The temperature of the faster component reached about 3000 K at 45° and rapidly decreased with increasing desorption angle. The inclined component involved the highest-energy component of desorbing oxygen.

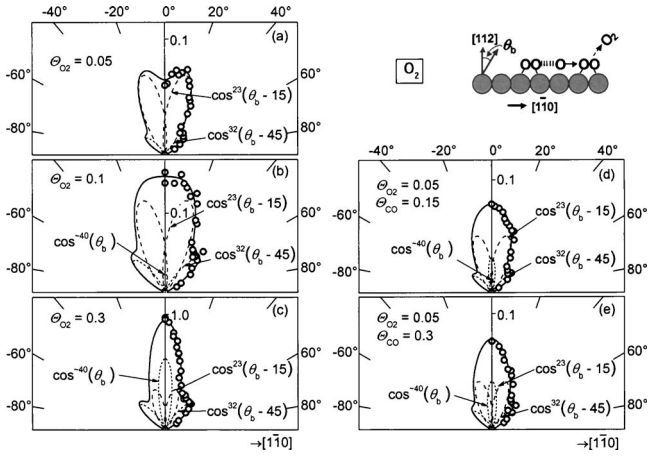

FIG. 2. Angular distributions of oxygen desorbed by 193-nm irradiation in the plane along the surface trough. (a) 0.05-ML O_2, (b) 0.1-ML O_2, (c) 0.3-ML O_2, (d) 0.05-ML O_2+0.15-ML $^{13}C\,^{18}O$, and (e) 0.05-ML O_2+0.3-ML $^{13}C\,^{18}O$. The signal on the ordinate was normalized to that in the normal direction in (c). Typical deconvolutions are shown by broken curves. A side view of Pt(112) along the surface trough and a collision mechanism are shown on the top.

O_2 desorption below 0.1-ML O_2 was concentrated in the plane along the surface trough. The angle θ_b dependence of the flux peaked at around 15° at $\Theta_{O_2}=0.05$ ML [Fig. 2(a)]. Considering the above velocity analysis and the surface symmetry, the angular distribution was resolved into two sets of the power series of $\cos^{23}(\theta_b+15)+\cos^{23}(\theta_b-15)$ and $\cos^{32}(\theta_b+45)+\cos^{32}(\theta_b-45)$. Increasing the O_2 coverage to 0.1 ML, both components were enhanced. A further increase in the oxygen exposure resulted in the relative enhancement of the component collimated at $\theta_b=45°$ [Fig. 2(c)]. On the other hand, another normally directed component, which was approximated as $\cos^{40\pm15}(\theta_b)$, was largely increased with increasing O_2 exposure and became significant at $\Theta_{O_2}=0.3$ ML. This component comes from the desorption collimated along the local normal of the (111) terrace. In fact, in the plane perpendicular to the surface trough, the O_2 desorption at 0.3-ML O_2 collimated close to the terrace normal as approximated to $0.35\cos^6(\theta_a+7)+\cos^9(\theta_a-15)$. The latter increased rapidly with increasing O_2 coverage above 0.15 ML and is due to the terrace component. The former comes from this plane component of the inclined desorption along the trough. The inclined desorption along the trough was actually in the plane shifted about 7° from the surface normal toward the step-down direction, i.e., $\theta_a=-7°$. Thus, the O_2 desorption was concluded to be split in four directional ways that collimated at $\theta_b=\pm14°-16°$ and $\pm44°-45°$ in the plane along the trough except for the high O_2 coverage range.

In the presence of $CO(a)$, the inclined O_2 desorption showed a similar angular distribution along the trough although the intensity was significantly decreased. The desorption was examined at 0.05-ML O_2 where the desorption

was merely collimated in the inclined way [Fig. 2(a)], whereas the terrace component became significant when 0.15-ML CO was coadsorbed [Fig. 2(d)]. At the presence of 0.3-ML CO, the inclined component decreased to about 60% [Fig. 2(e)]. Instead, the normally directed component desorbed from the (111) terrace was enhanced, suggesting that CO pushed oxygen molecules from steps to the terrace.

C. CO_2 desorption

The CO_2 desorption at small O_2 coverage was enhanced along the trough in the plane slightly shifted from the normal in a similar way to the O_2 desorption. This shift was only 7°–10° toward the step-down direction. At $\Theta_{O_2}=0.05$ ML and $\Theta_{CO}=0.09$ ML, the intensity in the plane perpendicular to the trough was described as $0.13\cos^{20}(\theta_a+10)+0.04\cos^{40}(\theta_a-18)$ [Fig. 3(b)]. In the plane along the trough, the desorption collimated at around $\theta_b=21°$ from the normal, as approximated in a form of $0.13\cos^{16}(\theta_b-21)+0.13\cos^{16}(\theta_b+21)$ [Fig. 3(a)]. With increasing oxygen coverage, the CO_2 desorption along the (111) terrace normal largely increased as approximated in a form of $\cos^{40}(\theta_a-18)$ [Fig. 3(c)].

A typical velocity distribution of CO_2 is shown at $\theta_b=30°$ [Fig. 4(a)]. The distribution is accompanied with another hyperthermal component above 2 km s^{-1}. The curve was deconvoluted into two modified Maxwell forms as shown by the broken lines. The faster component, whose temperature was maximized to 6230 K, collimated sharply at $\theta_b=29°$. Its flux was approximated in a $\cos^{70\pm15}(\theta_b-29)$ form. The remaining component, which was major and showed a translational temperature of about 2650 K, collimated at $\theta_b=20°$. The flux was approximated in a $\cos^{16}(\theta_b-20)$ form. Thus, the CO_2 desorption is also split in a multidirectional way collimated at $\theta_b=\pm29°$ and ±20° in a plane along the trough [Fig. 3(a)].

IV. DISCUSSION

A. Inclined desorption components

The product desorption collimated at two different directions in the plane along the surface trough. For O_2 desorption, the collimation was at $\theta_b=44°-45°$ with a maximum temperature of 3000 K and along $\theta_b=14°-16°$ with a maximum temperature of 1850 K. The desorption that collimated around $\theta_b=14°-16°$ was dominant below $\Theta_{O_2}=0.17$. Above it, the component that collimated at $\theta_b=44°-45°$ was enhanced. This component was noticeable even at $\Theta_{O_2}=0.05$. For CO_2 desorption, the collimation was at $\theta_b=29°$ with a maximum $T_{\langle E\rangle}$ value of 6230 K and along $\theta_b=20°$ with $T_{\langle E\rangle}=2650$ K. Commonly, the component with a larger collimation angle shows higher kinetic energy. These inclined desorptions are induced by hot-atom oxygen emitted from O_2 molecules aligned along the trough. In fact, the O–O axis was confirmed to be oriented along the trough on this surface at around 100 K in a wide coverage range by near-edge x-ray-absorption fine structure (NEXAFS).[29] Later, these O_2 molecules were confirmed to be located on the fringe of the terrace by STM.[36] This is also consistent with the infrared reflection absorption spectroscopy (IRAS) work reported by Tripa and Yates, according to which, on Pt(112), oxygen first occupies step sites and above 0.2 ML, starts to adsorb on the terrace.[37]

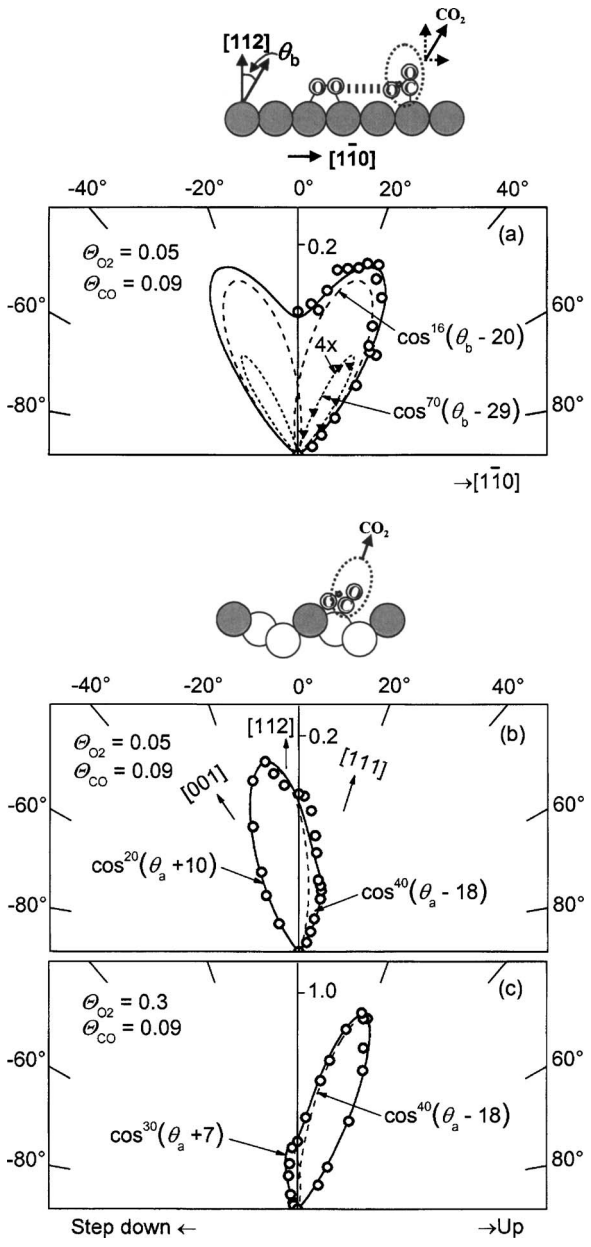

FIG. 3. (a) Angular distributions of desorbing $^{13}C\ ^{18}O\ ^{16}O$ in the normally directed plane along the trough at 0.05-ML $^{16}O_2$+0.09-ML $^{13}C\ ^{18}O$. The fastest components derived from the velocity distribution analysis are shown by closed triangles. The remaining fast components are drawn by broken curves. The open circles show the observed total flux. The solid line stands for their summation. A side view of Pt(112) along the surface trough and a collision-inducing desorption mechanism are shown on the top. (b) and (c) Angular distribution of $^{13}C\ ^{16}O\ ^{18}O$ in the plane perpendicular to the trough. $^{16}O_2$ was first dosed and then 0.09-ML $^{13}C\ ^{18}O$ was adsorbed. Typical deconvolutions are drawn by broken curves. A side view of the terrace sites is shown on the top.

The O_2 desorption in the plane along the trough is merely described as the inclined desorption induced by hot-atom oxygen collision, in high contrast with the results on Ag(110), which yield the major desorption along the surface normal.[18,19] The latter normally directed desorption was ex-

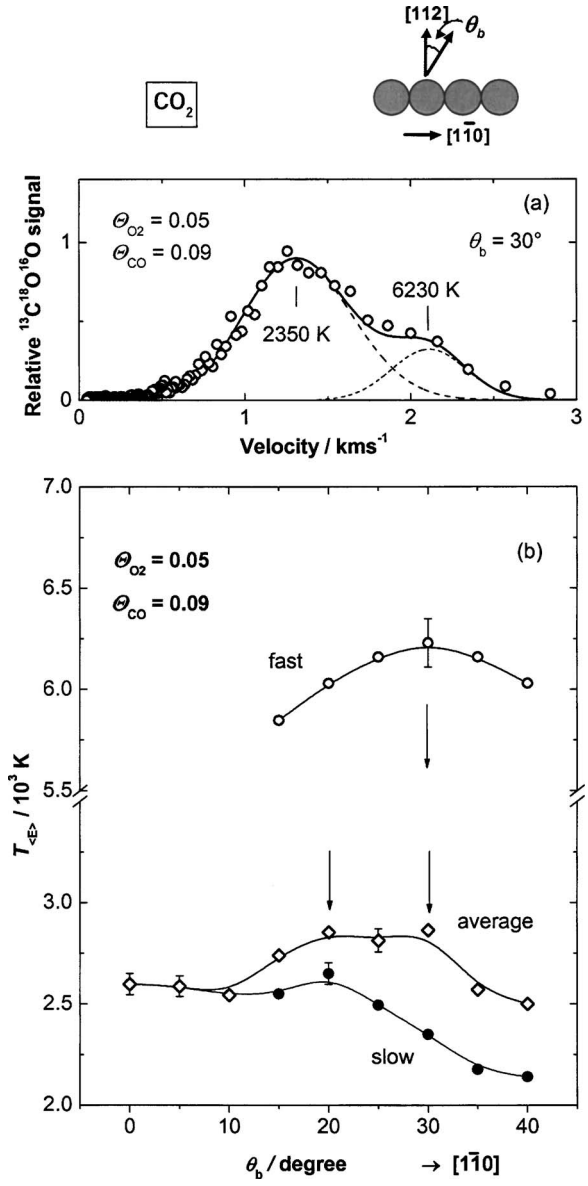

FIG. 4. (a) Velocity distribution of desorbing ^{13}C ^{18}O ^{16}O at θ_b=30° in the plane along the surface trough at 0.05-ML $^{16}O_2$+0.09-ML ^{13}C ^{18}O. A typical deconvolution is drawn by broken curves. The translational temperature of each component is inserted. (b) Translational temperatures versus the desorption angle in the plane along the surface trough at the conditions of (a). Each component was described in the text.

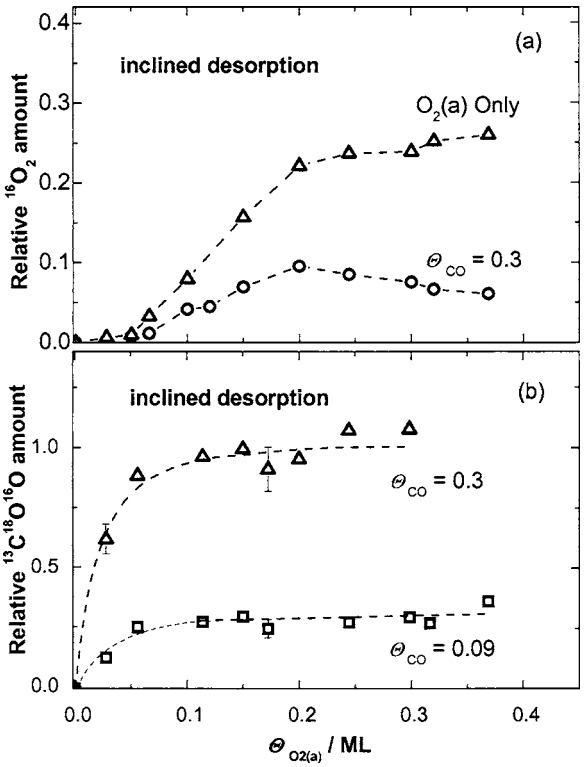

FIG. 5. Variation of the integrated amounts of (a) O_2^{16} and (b) $C^{13}O^{18}O^{16}$ desorbed in the inclined way with the O_2 coverage. Remarkable differences are seen in the initial increase between O_2 and CO_2.

plained by either Antoniewicz mechanism or the charge-withdraw mechanism, without collision of hot atoms.[38,39]

B. Reaction cross sections of CO and O_2

The total amount of each desorbed component along the trough was estimated from the AR-signal intensity at the collimation angle, the sharpness of the angular distribution around the collimation axis, and the QM sensitivity correction.[40] The results are plotted against the O_2 coverage in Fig. 5. On the surface covered by only O_2, the O_2-inclined desorption along the trough increases above 0.05-ML O_2 with increasing coverage and reaches a steady value around Θ_{O_2}=0.2 ML. The step metal site is fully occupied by O_2 at Θ_{O_2}=0.17 ML when O_2 preferentially occupies step atoms. The initial induction coverage suggests the presence of the minimum coverage needed to start the inclined O_2 desorption. This is probably due to the situation that the transfer distance of hot-atom oxygen is not enough to induce the desorption. In fact, the inclined CO_2 desorption starts immediately, i.e., there was no induction coverage and the initial slope of the inclined CO_2 desorption was proportional to the CO coverage [Fig. 5(b)]. This indicates that O_2 emits hot atoms that attack neighbor CO molecules, yielding CO_2 with a high probability. In fact, the desorption probability of CO_2 was estimated to be about six times higher than that of O_2. For example, at 0.05-ML O_2 and 0.09-ML CO, the initial desorption ratio of CO_2/O_2 was estimated to be about 15 from the data in Fig. 5. This value decreases to about 5 if the same O_2 desorption yield as that without CO(a) is assumed. A similar explanation was given from the IRAS observation of the decrement of CO(a) by Tripa and Yates.[37]

Both desorbed CO_2 and O_2 showed two components collimated at different angles. The amount of the faster CO_2 component was estimated to be only 1/40 of the slower one in the same analysis procedure as above. A similar situation was also found for O_2, where the faster was about 1/10 of the slower component. The results as well as the other desorption parameters are listed in Table I. The yield of the faster component with higher energy is commonly smaller, consistent with the MD results on Ag(110).[26,27] The reaction cross section may decrease with increasing kinetic energy of the reactant when the activation energy for the reaction is small.[41]

The inclined O_2 desorption is highly suppressed in the presence of CO(a) and reaches only about one-fourth of that without CO(a). Two factors may be operative. First, CO(a)

TABLE I. Desorption parameters of each component at 193 nm.

	Desorbing product				Relative yield[a]		Hot-atom[b] (eV)	Normal repulsion[c] (eV)	
	Collimation angle (degree)		Distri. sharpness $\cos^n\theta$	Maximum energy. (eV)	comp.	total	parallel	step	terrace
CO_2	fast	29	$n=70$	1.1 (6200 K)	1	6	0.75	0.70	0.56
	slower	20	16	0.46	40	···	0.15	0.42	
O_2	fast	45	32	0.52	1	1	0.60	0.27	0.30
	slower	15	21	0.32	10	···	0.05	0.25	

[a]The ratio of the amount of fast to slower component derived from angular distributions.
[b]The hot-atom energy estimated from the surface parallel velocity component of desorbing products at the collimation angle.
[c]The energy derived from the normal velocity component of desorbing products at the collimation angle in the inclined (step) and terrace components.

can reduce the number of oxygen molecules aligning along the step edge because of the higher adsorption energy over O_2. Second, CO(a) can receive more hot-atom oxygen than that needed for the collision to O_2(a) since it is highly reactive to atomic oxygen before being stabilized. Mullins *et al.* observed a high yield of CO_2 from CO-covered Pt(111) at 90 K by introducing oxygen atom beams.[42] Hot-atom oxygen emitted from O_2 can react with CO on Pt(111) even at T_S around 30 K.[43,44] The activation barrier is low for the reaction between adsorbed CO and hot-atom oxygen, i.e., adsorbed CO has a large reaction cross section towards hot-atom oxygen with less kinetic energy. On the other hand, there might be significant activation energy for O_2 desorption since its adsorption bond must be broken without a chemical reaction to the hot atom.[27] This will explain why there is less energy dependence on the O_2 desorption cross section.

In the gaseous reaction of a singlet state oxygen atom (^1D) with CO, no activation energy is expected although the released energy must be dissipated for stable CO_2 formation.[45] On the other hand, the reaction of a triplet state oxygen atom (^3P) with CO has small activation energy, around 0.25 eV.[46]

C. Terrace components

At O_2 coverage higher than 0.17 ML, the reactive CO_2 desorption was highly enhanced along the (111) terrace normal. At 0.3-ML O_2 and 0.09-ML CO, the terrace component reached about 70% of that in the plane along the trough. This indicates that oxygen admolecules also populate the terrace above 0.17 ML. The appearance of the terrace components only at high O_2 coverage does not necessarily mean the operation of a different reaction mechanism although the translational temperature of CO_2 from the (111) terrace is 2500 K below half that of the fastest component in the inclined desorption. Rather, the same hot-atom collision mechanism is still operative, but the hot-atom momentum is not directly transferred into the product desorbing along the terrace normal. Oxygen admolecules on the terrace plane can induce reactive desorption along the terrace normal and not necessarily along the trough. In this desorption process, no direct momentum transfer of hot-atom oxygen to desorbing products is expected. This is because the hot-atom movement is perpendicular to the trajectory of the product. The desorbing product is likely to be accelerated by the repulsive part of the potential energy of CO_2 (or O_2) adsorption, which is frequently observed in the thermal CO oxidation. The translational temperature of desorbing CO_2 along the terrace normal is 2500 K, much higher than that in the thermal CO oxidation (ca. 1400 K).[47,48] This may be due to the rapid formation of bulky molecules close to the surface, inducing more repulsive forces from the surface, i.e., the transition state is formed deeply in the repulsive part of its physical adsorption potential of CO_2.[1] The reacting hot-atom oxygen is coalesced into producing CO_2 and its momentum along the normal direction must be received from the surface. For O_2 desorption, the conditions are slightly different; the terrace desorption component had a translational temperature of 1600–1700 K. The repulsion from the surface is less than that for CO_2 because of the smaller size.

The above consideration provides information on the repulsive forces operative toward the nascent products from the surface without a direct contribution of the momentum transfer from the hot-atom oxygen. This is useful to analyze the collision-induced desorption in the next chapter. The above repulsive desorption also proposes another mechanism for desorbing O_2 and CO_2 collimated along the surface normal in photoinduced reactions on Pt(111) and Ag(110),[15,18,19] and their kinetic energy is less than that in the inclined desorption. This is neither Antoniewicz mechanism nor the charge-withdraw mechanism,[38,39] and it is induced by hot-atom oxygen in a peculiar momentum transfer.

D. Collision-induced desorption

These multidirectional components are reminiscent of O_2 desorption at 193 nm on Pt(113)(1×2), on which the desorption collimated at $\theta_b=12°-20°$ and $\theta_b=45°-49°$.[21]

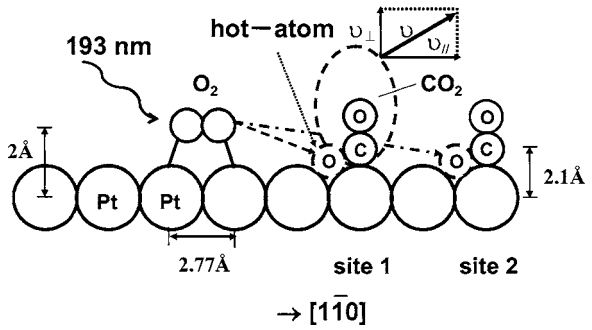

FIG. 6. A model of hot-atom oxygen reaction. The distance of O_2 (a) to metal atoms is referred to the structure of metal complex involving O_2. The size of CO_2 is drawn by assuming van der Waals' radii. Its velocity is divided into surface parallel and perpendicular components. Typical nearest (Site 1) and second nearest sites (Site 2) are shown for CO_2 formation.

These inclined collimations were discussed in the framework of a hard-sphere inelastic collision model, i.e., the desorption of oxygen molecules should be collimated at the angle of $\rho = \cos^{-1}(b/d)$, where b is the impact parameter and d is the collision diameter.[49] Very similar collimation angles were observed on the present surface, indicating that the same mechanism is operative along the trough with different step structures. The collimation angles of 14°–16° and 44°–45° require impact parameters of $b = \sim 2.0$ and ~ 1.5 Å. These values are not unreasonable because the admolecule seems to be located further from the surface, probably about 2 Å,[50] and oxygen adatoms are 0.85 Å above the platinum plane (Fig. 6).[51] Actually, hot-atom oxygen will move towards the surface as well as along the trough, yielding larger b values. Thus, at high coverage, collision with smaller impact parameters becomes possible because the distance between neighboring admolecules becomes shorter, yielding desorption at larger desorption angles.

However, this hard-sphere collision model is too simple because it is not suitable to examine the kinetic-energy effect toward the collimation angle and the reaction cross section. The present observations must be explained from the kinetic-energy point of view. The kinetic energy of hot-atom oxygen is quickly dissipated due to surface corrugations as it proceeds along the trough.[27] In fact, hot atoms emitted from O_2 are mostly stabilized a few atoms far from the dissociation place.[36,52] The energy is too high toward the reaction with the nearest-neighbor species and largely decreases with the next-nearest species where the energy is more suitable for the reaction. The collision with hot-atom oxygen with very high energy at a shorter distance will yield desorption in the inclined way closely parallel to the surface plane.

This is in high contrast to Zeiri's MD simulations for collision-induced O_2 desorption on Ag(110) at 248-nm laser light.[26] He predicted two desorption components. At low O_2 density (around 0.25 ML), the main desorption is induced by a single hot-atom collision, yielding a component collimated at 60°–80° from the surface normal and a kinetic energy of 0.1–0.2 eV. The minor desorption broadly collimates at 20°–50°. The latter is induced by the secondary collision toward the O_2 behind the target molecule and becomes major at high O_2 density. In the present case, the O_2 desorption component at 44° with high energy increased with increasing coverage. On the other hand, the component at 14°–16° with less energy relatively decreased at high coverage. This indicates that two inclined O_2 desorption components are induced by different distances/hot-atom energy, and not simply by different O_2 densities. The situation became clearer with desorbing CO_2. There are two collimated components, i.e., one at 29° with 6200 K and the other at 20° with 2650 K (Fig. 6). The former component is induced by hot-atom oxygen with higher energy as judged from the large collimation angle, smaller reaction cross section, and high kinetic energy of desorbing CO_2. This component was observed at wide coverage of CO(a) and O(a). It was significant even when the step Pt atoms were mostly occupied by either CO or O_2. This component is likely to desorb without being scattered by the next neighbor behind the target.

E. Energetics

In the simple collision mechanism, poor energy transfer from hot-atom oxygen to desorbing O_2 is expected because heavy O_2 moving along inclined directions cannot efficiently receive kinetic energy. In fact, the kinetic energy of desorbing O_2 in the above MD simulation was only 0.15 eV although the initial energy of hot atom was estimated to be about 1 eV.[26] However, the desorbing O_2 actually held high kinetic energy, 0.53 eV (3000 K). Thus, another energy-transfer channel must be operative in the desorption event. This situation is remarkable for desorbing CO_2 since the CO_2 component directed to 29° showed a very sharp collimation and its translational temperature reached 6230 K (1.1 eV). The second inclined CO_2 component showed 2650 K (0.46 eV) at $\theta_b = 20°$. These translational temperatures of CO_2 in the inclined desorption are almost twice that of O_2. However, their collimation angles are not larger than those of O_2. There must be a mechanism in which desorbing CO_2 can receive more repulsive forces towards the surface normal from the surface than O_2.

Here we estimate the kinetic energy of hot-atom oxygen from the collimation angle and the kinetic energy of desorbing products, assuming simply the momentum conservation in the collision event. The momentum of desorbing CO_2 (or O_2) is divided into the surface-parallel and -perpendicular components and the former is assumed to be preserved during collision. The resultant kinetic energy of the hot atom is listed in the right column of Table I. The kinetic energy of a hot atom estimated at the nearest site is 0.6–0.75 eV commonly from CO_2 and O_2 as expected. The value at the next site is 0.05–0.15 eV. This is probably the average value over the sites after the second because the reaction cross section of CO toward hot-atom oxygen is large enough to accept slower atoms even at the third site and thereafter. The distribution of the second desorption component is broad and overlapped with the fast one, as a result, it is not deconvoluted. Therefore, the energy difference, 0.5–0.6 eV, might be overestimated as the energy decrease from the first to the next site. Thus, about 1 eV is the upper limit of the hot-atom energy immediately after O_2 dissociation. This value agrees well with the results at 248 nm.[18] The kinetic energy of a hot atom is not directly related to the excitation light wave

number because the energy state of $3\sigma^*$ orbital of $O_2(a)$ is broad on the metal surface and the energy states involved in the excitation may depend on the wave number.[16]

Both products received repulsive forces along the surface normal. The extent was estimated to be 0.42–0.70 eV for CO_2 and 0.25–0.27 eV for O_2. The hot-atom oxygen cannot transfer the momentum along the surface normal without a special conversion mechanism. In particular, CO_2 receives high repulsive forces from the surface. This momentum transfer is very similar to that in the terrace component which is repulsed from the terrace without direct momentum transfer from hot-atom oxygen. The value is 0.56 eV for CO_2 and 0.30 eV for O_2 (Table I). These values agree well with those derived from the normal component of the inclined desorption. It is noteworthy that the kinetic energy of desorbing CO_2 is higher than that of the hot atom although the internal energy is ignored. This indicates a significant contribution from the heat of CO_2 formation. Eventually, the lifetime of a hot atom was estimated to be in the order of 10^{-13} s.

The small reaction cross section at the nearest site is common for CO_2 formation and O_2 desorption. In particular, the reaction cross section toward CO at the nearest site is very small. Hot-atom oxygen can hardly form CO_2 when its kinetic energy is higher than 1 eV. In Zeiri's MD work,[26] the reaction cross section toward the nearest O_2 was estimated to be about one-tenth of that of the next-nearest O_2 when the initial kinetic energy of the hot atom was 1 eV (or above this value). This is very close to the present results.

In the above energy estimation, no directed momentum transfer is assumed along the surface normal, i.e., perpendicular to the hot-atom trajectory. The repulsive forces exerted from the surface would be overestimated when the momentum is directly transferred. Such a transfer is expected in the above hard-sphere inelastic collision model where the hot-atom collision induces rotational motions of the target molecule by hitting its metal-side end. The effect due to this mechanism was evaluated on Ag(110) in Zeiri's MD simulations. The resultant energy was very small.[26]

V. CONCLUSIONS

The photodesorption of oxygen and CO_2 was studied in $CO+O_2$ coadsorption layers on Pt(112) by using an ArF Excimer laser (193 nm). The results are summarized as follows:

(1) Multidirectional O_2 desorption, collimated at 14°–16° and 44°–45° off the surface normal, is found in a plane along the trough. At high O_2 coverage, O_2 desorption also takes place along the (111) terrace normal.
(2) CO_2 desorption also shows multidirectional ways, collimated at 20° and 29° off the surface normal along the trough. At high O_2 coverage, CO_2 desorption collimates sharply along the (111) terrace normal. The cross section of CO towards hot atom was found to be higher than that of O_2.
(3) The multidirectional desorption is commonly explained by a simple collision-induced desorption model.

ACKNOWLEDGMENTS

One of the authors (S. H.) is indebted to the Clark Memorial Foundation and the Ministry of Education, Science, Sports, and Culture of Japan for their scholarships. The authors thank Hiratsuka for drawing the figures. This work was partly supported by Grant-in-Aid No. 13640493 for General Scientific Research from the JSPS.

[1] T. E. Madey, D. E. Ramaker, and R. Stockbauer, Annu. Rev. Phys. Chem. **35**, 215 (1984).
[2] R. H. Stulen, Prog. Surf. Sci. **32**, 1 (1989).
[3] R. D. Ramsier and J. T. Yates, Jr., Surf. Sci. Rep. **12**, 243 (1991).
[4] J. V. Barth, Surf. Sci. Rep. **40**, 75 (2000).
[5] T. Matsushima, Surf. Sci. Rep. **52**, 1 (2003).
[6] M. P. D'Evelyn and R. J. Madix, Surf. Sci. Rep. **3**, 413 (1984).
[7] G. Comsa and R. David, Surf. Sci. Rep. **5**, 145 (1985).
[8] T. Matsushima, Heterog. Chem. Rev. **2**, 51 (1995).
[9] Y. Ohno, K. Kimura, M. Bi, and T. Matsushima, J. Chem. Phys. **110**, 8221 (1999).
[10] H. Horino, S. Liu, A. Hiratsuka, Y. Ohno, and T. Matsushima, Chem. Phys. Lett. **341**, 419 (2001).
[11] H. Horino, I. I. Rzeznicka, A. Kokalj, I. Kobal, A. Hiratsuka, Y. Ohno, and T. Matsushima, J. Vac. Sci. Technol. A **20**, 1592 (2002).
[12] K. Imamura, H. Horino, I. I. Rzeznicka *et al.*, Surf. Sci. **566/568**, 1076 (2004).
[13] K. Imamura and T. Matsushima, Catal. Lett. **97**, 197 (2004).
[14] T. Matsushima, I. I. Rzeznicka, and Y.-S. Ma, Chem. Rec. **5**, 81 (2005).
[15] W. D. Mieher and W. Ho, J. Chem. Phys. **99**, 9279 (1993).
[16] X.-Y. Zhu, S. R. Hatch, A. Campion, and J. M. White, J. Chem. Phys. **91**, 5011 (1989).
[17] X.-Y. Zhu, J. M. White, M. Wolf, E. Hasselbrink, and G. Ertl, Chem. Phys. Lett. **176**, 459 (1991).
[18] Q.-S. Xin and X.-Y. Zhu, Surf. Sci. **347**, 346 (1996).
[19] X.-Y. Zhu, Surf. Sci. **390**, 224 (1997).
[20] J. Stöhr, J. L. Gland, W. Eberhardt, D. A. Outka, R. J. Madix, F. Sette, R. J. Koestner, and U. Doebler, Phys. Rev. Lett. **51**, 2414 (1983).
[21] M. Sano, Y. Ohno, T. Yamanaka, T. Matsushima, E. B. Quinay, and K. Jacobi, J. Chem. Phys. **108**, 10231 (1998).
[22] T. Yamanaka, Y. Inoue, and T. Matsushima, J. Chem. Phys. **110**, 2597 (1999).
[23] T. Yamanaka, T. Matsushima, S. Tanaka, and M. Kamada, Surf. Sci. **349**, 119 (1996).
[24] A. Kose and D. A. King, Chem. Phys. Lett. **313**, 1 (1999).
[25] T. Yamanaka, Q. K. Xue, K. Kimura, T. Matsushima, Y. Hasegawa, and T. Sakurai, Jpn. J. Appl. Phys., Part 1 **39**, 3562 (2000).
[26] Y. Zeiri, J. Chem. Phys. **112**, 3355 (2000).
[27] M. Asscher and Y. Zeiri, J. Phys. Chem. B **107**, 6903 (2003).
[28] A. Szabó, M. A. Anderson, and J. T. Yates, Jr., J. Chem. Phys. **96**, 6191 (1992).
[29] S. Wako, M. Sano, Y. Ohno, T. Matsushima, S. Tanaka, and M. Kamada, Surf. Sci. **461**, L537 (2000).
[30] H. Horino, S. Liu, M. Sano, S. Wako, A. Hiratsuka, Y. Ohno, I. Kobal, and T. Matsushima, Top. Catal. **18**, 21 (2002).
[31] T. Matsushima, Surf. Sci. **127**, 403 (1983).
[32] S. S. Mann, B. D. Todd, J. T. Stuckless, T. Seto, and D. A. King, Chem. Phys. Lett. **183**, 529 (1991).
[33] S. R. Hatch, X.-Y. Zhu, J. M. White, and A. Campion, J. Phys. Chem. **95**, 1759 (1991).
[34] A. Winkler, X. Guo, H. R. Siddiqui, P. L. Hagans, and J. T. Yates, Jr., Surf. Sci. **201**, 419 (1988).
[35] I. I. Rzeznicka, Y.-S. Ma, G. Cao, and T. Matsushima, J. Phys. Chem. B **108**, 14232 (2004).
[36] B. C. Stipe, M. A. Rezaei, and W. Ho, J. Chem. Phys. **107**, 6443 (1997).
[37] C. Emil Tripa and J. T. Yates, Jr., Nature (London) **398**, 591 (1999).
[38] P. R. Antoniewicz, Phys. Rev. B **21**, 3811 (1980).
[39] C. T. Rettner and J. Lee, J. Chem. Phys. **101**, 10185 (1994).
[40] G. Cao, Md. G. Moula, Y. Ohno, and T. Matsushima, J. Phys. Chem. B **103**, 3235 (1999).
[41] S. T. Ceyer, Annu. Rev. Phys. Chem. **39**, 479 (1988).
[42] C. B. Mullins, C. T. Rettner, and D. J. Auerbach, J. Chem. Phys. **95**, 8649 (1991).
[43] R. A. Pelak and W. Ho, Surf. Sci. **321**, L233 (1994).

[44] J. Yoshinobu and M. Kawai, J. Mol. Catal. A: Chem. **141**, 57 (1999).
[45] D. R. Harding and R. E. Weston, Jr., J. Chem. Phys. **88**, 3590 (1988).
[46] M. Braunstein and J. W. Duff, J. Chem. Phys. **112**, 2736 (2000).
[47] A. Rar, H. Sugimura, A. Barrera, Y. Ohno, and T. Matsushima, Surf. Sci. **348**, 77 (1996).
[48] Y. Ohno, A. Barrera, A. Rar, T. Yamanaka, H. Sugimura, and T. Matsushima, Surf. Sci. **357/358**, 786 (1996).
[49] R. D. Levine R. B. Bernstein, in *Molecular Reaction Dynamics* (Oxford University Press, Oxford, 1974), p. 49.
[50] L. Vaska, Acc. Chem. Res. **9**, 175 (1976).
[51] K. Mortensen, C. Klink, F. Jensen, F. Besenbacher, and I. Stensgaard, Surf. Sci. **220**, L701 (1989).
[52] J. Wintterlin, R. Schuster, and G. Ertl, Phys. Rev. Lett. **77**, 123 (1996).